Evolution of a *cis*-acting SNP that controls Type VI Secretion in *Vibrio cholerae*

Siu Lung Ng[1,3,4], Sophia Kammann[1,3,4], Gabi Steinbach[2,4], Tobias Hoffmann[1,3], Peter J Yunker[2,4], Brian K. Hammer[1,3,4#]

[1] School of Biological Sciences, Georgia Institute of Technology, Atlanta, Georgia, USA

[2]School of Physics, Georgia Institute of Technology, Atlanta, Georgia, USA

[3]Parker H. Petit Institute for Bioengineering & Bioscience, Georgia Institute of Technology, Atlanta, Georgia, USA

[4]Center for Microbial Diseases and Infection, Georgia Institute of Technology, Atlanta, Georgia, USA

#Corresponding author: brian.hammer@biology.gatech.edu

Running title: Evolution of the *V. cholerae* T6SS by a *cis*-acting SNP

Abstract

Mutations in regulatory mechanisms that control gene expression contribute to phenotypic diversity and thus facilitate the adaptation of microbes and other organisms to new niches. Comparative genomics can be used to infer rewiring of regulatory architecture based on large effect mutations like loss or acquisition of transcription factors but may be insufficient to identify small changes in non-coding, intergenic DNA sequence of regulatory elements that drive phenotypic divergence. In human-derived *Vibrio cholerae,* the response to distinct chemical cues triggers production of multiple transcription factors that can regulate the Type VI Secretion System (T6), a broadly distributed weapon for interbacterial competition. However, to date, the signaling network remains poorly understood because no regulatory element has been identified for the major T6 locus. Here we identify a conserved *cis*-acting single nucleotide polymorphism (SNP) controlling T6 transcription and activity. Sequence alignment of the T6 regulatory region from diverse *V. cholerae* strains revealed conservation of the SNP that we rewired to interconvert *V. cholerae* T6 activity between chitin-inducible and constitutive states. This study supports a model of pathogen evolution through a non-coding *cis*-regulatory mutation and preexisting, active transcription factors that confers a different fitness advantage to tightly regulated strains inside a human host and unfettered strains adapted to environmental niches.

Importance

Organisms sense external cues with regulatory circuits that trigger the production of transcription factors, which bind specific DNA sequences at promoters ("*cis*" regulatory elements) to activate target genes. Mutations of transcription factors or their regulatory elements create phenotypic diversity, allowing exploitation of new niches. Waterborne pathogen *Vibrio cholerae* encodes the Type VI Secretion System "nanoweapon" to kill competitor cells when activated. Despite identification of several transcription factors, no regulatory element has been identified in the promoter of the major Type VI locus, to date. Combining phenotypic, genetic, and genomic analysis of diverse *V. cholerae* strains, we discovered a single nucleotide polymorphism in the Type VI promoter that switches its killing activity between a constitutive state beneficial outside hosts and an inducible state for constraint in a host. Our results support a role for non-coding DNA in adaptation of this pathogen.

Introduction

A central role in the dynamic, temporal control of gene expression is played by transcription factors (TFs), diffusible "*trans"* products that bind to molecular switches within DNA sequences termed "*cis"*-regulatory elements (CREs). In eukaryotes, where horizontal gene transfer (HGT) is rare, mutations in CREs that alter TF binding sites are major contributors to

phenotypic diversity (1-3). In bacteria, pervasive HGT can alter entire regulatory circuits that allow adaptation to new niches, as prominently demonstrated in *Vibrio fischeri*, where host range is altered by the presence or absence of a histidine kinase RcsS, which regulates biofilm and colonization genes via indirect mechanisms (4, 5). By contrast, specific mutations at CREs in non-coding DNA are more difficult to identify and receive less attention as drivers of phenotypic divergence and evolutionary adaptation (6). Thus, elucidation of how microbes adapt to new niches, a process of fundamental importance in bacterial pathogenesis, requires coupling of genome-wide computational methods with experimental approaches to map the *cis*- and *trans*-regulatory interactions across and within species.

To understand how mutations play a role in microbial adaptation, pathogenic viruses and bacteria with lifestyles that exploit niches within and outside a human host are of great interest. Following ingestion, pandemic strains of the bacterium *Vibrio cholerae* can colonize the human gastrointestinal tract and secrete the cholera toxin that leads to the often fatal diarrhea responsible for seven pandemics to date (7-9). Conversely, *V. cholerae* isolated from non-human niches lack the horizontally-acquired prophage that carries the cholera toxin, and cause mild illness (10). By contrast, all sequenced *V. cholerae* encode a Type VI Secretion System (T6), a broadly distributed “nano-harpoon” weapon that injects toxic effector proteins into neighboring bacterial cells, leading to cell envelope damage and cell lysis (11, 12). Due to

its broad distribution among bacteria including those of the human gut, there is intense interest in understanding the T6 interactions between our microbiota and foreign pathogens, and whether they can be manipulated to influence health (13).

V. cholerae obtained from humans carry a limited arsenal of effectors and a T6 believed to be tailored for *in vivo* success (11, 14-19), while strains from non-human niches encode a more diverse effector repertoire (11, 14, 20, 21). To date, however, adaptative evolution mechanisms of T6 regulation in *V. cholerae* derived from non-human sources have largely been overlooked. Since the discovery of T6, studies of human-derived strains identify two primary TFs for T6 activation (22-26). T6 control in pandemic strains (e.g. C6706 and A1552) requires QstR, which is positively regulated by multiple external cues, including chitin that triggers TfoX production, and quorum-sensing autoinducers that control the well-studied LuxO/HapR regulatory circuit (27-30). QstR also contains a C-terminal DNA binding domain postulated to interact with a presumptive CRE of the major T6 gene cluster, yet how QstR-DNA interaction affects T6 transcription remains unclear (23, 27). On the other hand, T6 regulation in non-pandemic strain V52, which causes mild disease, requires TfoY, modulatable by intracellular signals, including cyclic di-GMP (25, 26). Over the past decade, the regulatory mechanisms of QstR and TfoY still remain unclear. Similarly, direct regulators of T6 transcription, still remain elusive, with only one putative T6 CRE described (23). Elucidation of

90 the differences in intraspecies T6 regulatory mechanisms between diverse *V. cholerae* isolates
91 will provide insights into how pathogens emerge from nonpathogenic progenitors.
92
93 To understand the regulatory differences in *V. cholerae* strains, we examine here several
94 environmental isolates that exhibit T6-mediated killing (31). Despite encoding functional
95 signaling circuity and TFs, we find that QstR is dispensable for killing and that TfoY plays only
96 a minor role in the strains tested. Thus, existing regulatory models fail to explain the T6
97 control in *V. cholerae* from human and non-human sources. Genomic analysis identifies one
98 conserved non-coding single-nucleotide polymorphism (SNP) that we show interconverts *V.*
99 *cholerae* T6 activity between chitin-inducible and constitutive states, which are QstR-
100 dependent and TfoY-independent, respectively. We demonstrate that non-coding SNPs can
101 rewire *cis*-regulatory elements to aid in adaptation of bacteria to different niches, including
102 the human host.
103
104 **Results and Discussion**
105 Constitutive, *in vitro* T6 activity requires neither QstR nor TfoY in many environmental *V.*
106 *cholerae* isolates.
107 In pandemic C6706, high cell density conditions (HCD) and chitin are required for induction of
108 *qstR* which leads to activation of T6 genes. In the absence of chitin, C6706 with *qstR* expressed

109 from a heterologous promoter (defined here as *qstR**) reduces survival of *Escherichia coli*
110 "target" cells in co-culture by over 4-orders of magnitude (~10,000), compared to wildtype
111 (WT) C6706, a T6^{-} strain with a mutation in an essential structural gene (*ΔvasK*), and a strain
112 with a *ΔqstR* mutation (Fig. 1A) (29). Deletion of *tfoY* does not reduce the killing activity of the
113 T6^{+} *qstR** strain, but eliminates the robust killing in the non-pandemic strain V52 (serogroup
114 O37), which requires TfoY but not QstR (Fig. 1B) (26).
115
116 To determine whether QstR or TfoY participates in control of the T6 in non-human derived
117 strains, we examined 3223-74, a genetically-amenable, T6-proficient environmental strain
118 (31). Like V52, 3223-74 does not require QstR to efficiently kill *E. coli* in conditions without
119 chitin, but surprisingly, also does not require TfoY. Isogenic strains carrying the *ΔtfoY* and
120 *ΔqstR ΔtfoY* mutations retain >99.99% killing activity, with only modest *E. coli* survival (Fig. 1C).
121 Gene fusions of the 5' intergenic region (IGR) of the major T6 cluster of each strain fused to
122 green fluorescent protein (*gfp*) confirm that transcriptional differences account for the killing
123 observed, with maximal *gfp* expression mirroring activity (i.e. low *E. coli* survival with high *gfp*
124 expression, and *vice versa*) (Fig. 1D-F). To confirm that expression of the major T6 loci is not
125 influenced by transcriptional read-through from a regulatory element upstream of the IGR, a
126 T7 terminator (32) was inserted directly after the stop codon of *vca0106* in *V. cholerae* with
127 activated T6 (Fig. S1). We observed no differences in T6 killing, demonstrating that the IGR is

sufficient for control of the major T6 locus. Confocal microscopy reinforces the negligible role of TfoY on killing by 3223-74, with a Δ*tfoY* mutation having little effect on killing WT (Fig. 1G). Transcription of plasmid-borne reporters is significantly higher in *V. cholerae* than in *E. coli* (Fig. S2), supporting a hypothesis that an additional *V. cholerae*-specific regulator of the T6 may remain to be identified.

To probe each strain's T6-related regulatory circuitry, we measured canonical behaviors under control of HapR, QstR and TfoY; quorum sensing (QS) controlled bioluminescence, natural transformation, and motility, respectively (33-35). As expected, each TF is intact in C6706; but like several *V. cholerae* strains, V52 lacks a functional *hapR* gene that prevents QS and natural transformation (36, 37). Nonetheless, V52 encodes a functional *tfoY* that controls motility (Fig. 2A-B) (38). Interestingly, the regulatory circuity of *V. cholerae* 3223-74 is intact, like C6706, confirming that it encodes functional TFs (Fig. 2C), which are nonetheless expendable for T6-mediated killing. Nucleoid Associated Proteins (NAPs) that bind DNA both specifically and non-specifically (39) may contribute to T6 transcription, since they are present in both species, likely regulated differently (40), and participate in regulation of many promoters in numerous bacteria including *Vibrios* (41). It is also possible that regulation may be complex, perhaps

involving more than one TF specific to *V. cholerae*.

A SNP in the T6 intergenic region confers QstR-dependency.

Human and environmental isolates of *V. cholerae* we have characterized prior (31) share ≥97% average nucleotide identity with many chromosomal differences (11), but inspection of the T6 IGRs of C6706, V52 and 3223-74 revealed only 17 SNPs and 3 multinucleotide polymorphisms (Fig. 3A), which we hypothesized could contribute to the differences in T6 transcription and killing activity observed. To address this, we replaced the T6 IGR of C6706 on the chromosome with that from V52 and 3223-74 and measured killing activity. While C6706 carrying the *qstR** allele, but not WT, adeptly kills *E. coli*, both IGR replacements increase the killing efficiency of WT C6706 by 5- to 6-orders of magnitude (Fig. 3B), mimicking the robust killing observed by WT V52 and 3223-74 (Fig. 1B-C). Deletion of *tfoY* but not *qstR* in C6706 with V52's IGR increases *E. coli* survival (~ 2-logs), as observed with V52, but does not alter *E. coli* survival with 3223-74's IGR (Fig. 3B, S3). Chromosomal transcriptional *gfp* reporters with identical mutations were elevated relative to WT C6706 in each IGR replacement strain (Fig. 3C), consistent with the enhanced killing detected. These results support a hypothesis that a novel CRE lies within the IGR 5' of the T6 locus, despite a lack of

any known direct TF-DNA interactions at this locus identified to date.

To begin mapping the T6 IGR region and SNP locations, we experimentally determined the transcriptional start site (+1) by 5' Rapid Amplification of cDNA Ends (Methods). The +1 of transcription resides 320 nucleotides (nt) 5' of the ATG of the first T6 gene (*vipA, vca0107*), and adjacent to a putative promoter with 8/12 identical nts compared to the consensus sigma70-dependent promoter (Fig. 3A). The +1 is consistent with paired-end RNAseq results we have reported prior (29). Because the majority of 5' untranslated regions (UTRs) in *V. cholerae* are 20-40 nt, with few exceeding 300 nt (42), we speculate that the 320 nt 5' UTR of the major T6 gene cluster may be post-transcriptionally regulated, beyond the sRNA interactions already described near the ribosome binding site (RBS) (43). Alignment of the IGRs of C6706 and V52 reveals a single SNP at -68, with a guanine (G) in C6706 at that position and a thymine (T) in V52 (Fig. 3A).

The replacement of the C6706 IGR with V52 was effectively a G-68T mutation (Fig. 3B-C), thus we further tested whether G was necessary for QstR activation by replacing the T with a G at position -68 (T-68G) in the 3223-74 WT, *qstR**, and *ΔqstR* backgrounds. The T-68G mutation significantly increases *E. coli* survival and decreases T6 transcription in WT 3223-74 and the *ΔqstR* derivative, with killing restored in the strain with the *qstR** allele (Fig. 3D-E). Thus, a G

181 at position -68 confers inducible, QstR-control, while a T results in constitutive killing *in vitro*,
182 consistent with results recently reported during manuscript revision (44). Based on these
183 results we predicted this SNP is a result of adaptive evolution to control T6 activity in different
184 environments.
185
186 The SNP at -68 is evolutionarily conserved.
187 To determine whether the SNP at -68 is prevalence in *V. cholerae*, we aligned the T6 IGR
188 sequences of diverse strains that we have characterized prior for T6 killing activity (Fig. 4A)
189 (31). Consistent with prior studies (11, 14, 16, 18), our phylogenetic analysis (Methods) of the
190 T6 IGRs places human strains in a distinct clade, with the exception of two O1 strains isolated
191 nearly a century ago (NCTC8457 and MAK757), and two non-O1 strains (MZO-2 O14 and V52
192 O37; Fig. S4). All 23 environmental isolates carry the T-68 SNP and displays constitutive T6
193 activity, with one exception that is chitin-inducible (1496-86) (Fig. 4A, S4). By contrast, the 18
194 human-derived isolates tested carry either G or T at the -68 position (Fig. 4A, S4). The 13
195 chitin-inducible human isolates carry a G; five show constitutive activity and carry a T like
196 environmental strains, with one exception that is constitutive yet carries the G (2010EL-1749)
197 (Fig. 4A, S4). Neither C nor A are observed at -68 in any stains tested, although both pyrimidine
198 nucleotides (T and C) confer constitutive killing at -68, and both purines (G and A) behave
199 similarly (Fig. S5). The focal SNP location is distal from the promoter, but inconsistent with AT-

200 rich “UP elements” that reside immediately upstream of the promoter at -38 to -59 and
201 interact directly with the alpha subunit of RNAP (45). We propose the SNP is more likely a
202 component of a CRE for a TF to be determined. Indeed, transversion mutations have greater
203 effects of TF binding than transitions, as noted here (Fig. S5) likely due to changes in shape of
204 the DNA backbone or DNA-amino acid contacts (46, 47).
205
206 We examined regulation of three additional genetically manipulatable environmental strains
207 (VC22, 2479-89, and 2512-86) that exhibit T6 killing (31). Like 3223-74, QstR is expendable in
208 each strain (Fig. 4B-E) while TfoY contributes to some extent in activating T6, with varying *E.*
209 *coli* recovery observed in each derivative carrying the *ΔtfoY* mutation (Fig. 4B-E). Taken
210 together, our findings reveal that the constitutive T6 killing activity of environmental *V.*
211 *cholerae* is driven by a T at position -68, which obviates the QstR requirement, and permits
212 modest TfoY regulation.
213
214 Bacterial adaptation to unexploited niches can be the result of horizontal gene transfer events
215 (5) as well as mutations in protein coding and promoter regions (48, 49). Here we describe an
216 intergenic non-coding SNP that coordinates adaptation by altering T6 control between two
217 states – one that in inducible and the other that displays constitutive activity. While the first
218 Type VI Secretion System was first described in *V. cholerae* in 2006, the knowledge of its

219 regulation remains largely restricted to human isolates

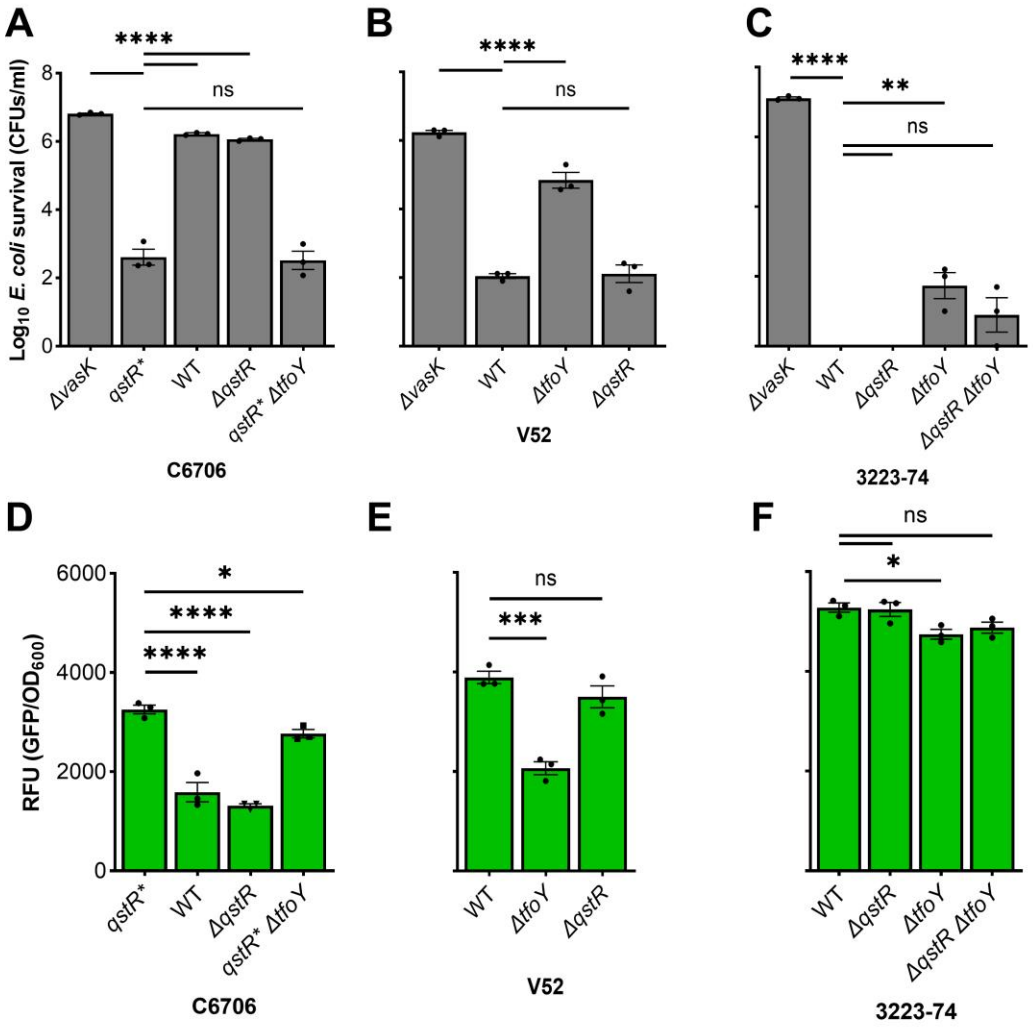
A
B
C
D
E
F
G
Log10 E. coli survival (CFUs/ml)
RFU (GFP/OD600)
ΔvasK
qstR*
WT
ΔqstR
qstR* ΔtfoY
ΔtfoY
ΔqstR ΔtfoY
C6706
V52
3223-74
ns
3223-74 ΔvasK
3223-74 ΔtfoY
0 h
3 h

220

221 incomplete, with the identity of a TF that directly controls the major T6 cluster elusive to this
222 date (22, 24). We speculate that the focal SNP we identified at position -68 is a component of
223 a CRE that contributes to pathoadaptation (Fig. 3A), a result of adaptive evolution, which
224 allows *V. cholerae* to carefully control the T6SS expression in specific environments. Our
225 results are consistent with the hypothesis that constitutive T6SS is beneficial in aquatic
226 environments outside a human host (50), with varying degrees of TfoY contribution, which
227 may act directly or indirectly at the transcriptional or posttranscriptional level (Fig. 3A and Fig.
228 4B-E, S6, S7). During human infection where selection promotes dampened T6SS, *V. cholerae*
229 with a T-to-G mutation (inducible T6) are favored. In fact, T6-deficient human isolates (e.g.
230 O395) have been reported to have less competitive fitness in human intestinal colonization
231 and infection (19, 51). Although low level, basal expression of T6 contributes to pathogenesis
232 of C6706 (52), overexpression of T6SS may be deleterious in vivo. Indeed, we have reported
233 prior that *V. cholerae* with constitutive T6SS induces violent peristaltic contractions in a fish
234 host (53), which may disrupt the interaction between *V. cholerae* and the gut microflora.
235
236 There remains a pressing public health need to understand the emergence of pathogens from
237 environmental reservoirs (54). Efforts such as Microbial Genome Wide Association Studies (55)
238 to identify genetic variants in genomes that are associated with phenotypes like virulence and
239 antibiotic sensitivity, will be bolstered by knowledge of the ecological and evolutionary

processes that promote pathogen-host association. Defining the plasticity of the regulatory circuity controlling the T6 weapon will provide insights into the role of polymorphisms in the evolution of this and other pathogens.

Materials and Methods

Bacterial growth conditions and plasmid constructions

All *V. cholerae* and *E. coli* (Table S1) strains were grown aerobically at 37 °C overnight in Lysogeny Broth (LB) with constant shaking or statically on LB agar. Ampicillin (100 μg/ml), kanamycin (50 μg/ml), chloramphenicol (10 μg/ml), spectinomycin (100 μg/ml), streptomycin (5 mg/ml), sucrose (20% w/v) and diaminopimelic acid (50 μg/ml) were supplemented where appropriate.

Plasmids (Table S2) used were constructed with DNA restriction nucleases (Promega – WI, USA), Gibson Assembly mix (New England Biolabs – MA, USA), and PCR amplification (Qiagen - Hilden, Germany) by PCR with Q5 polymerase (New England Biolabs – MA, USA), and primers (Table S3) generated by Eton Bioscience Inc (NC, USA) or Eurofins Genomics (KY, USA). All reagents were used according to the manufacturer's instructions. Plasmids were confirmed by PCR and Sanger sequencing by Eton Bioscience Inc (NC, USA).

V. cholerae mutant construction

All genetically engineered strains of *V. cholerae* were constructed with established allelic exchange methods using vector pKAS32 (56) and pRE118 (Addgene - Plasmid #43830). All Insertions, deletions, and mutations were confirmed by PCR and Sanger sequencing conducted by Eton Bioscience Inc (NC, USA). Primers used are in Table S3.

Fluorescence microscopy

V. cholerae 3223-74 strains and chromosomal-labeled GFP *E. coli* were separately back-diluted 1:100 and incubated at 37 °C for 3 h. *V. cholerae* and *E. coli* were normalized to OD_{600} = 1 and mixed in a 1:5 ratio. A 2 µL aliquot of a mixed culture was inoculated on LB agar and allowed to dry. Cells were imaged before and after a 3 h incubation at 37 °C and 96-100% humidity using an Eclipse Ti-E Nikon (NY, USA) inverted microscope with a Perfect Focus System and camera previously described (11). The images were processed with ImageJ (35).

Motility assay

Overnight cultures of *V. cholerae* were diluted to OD_{600} = 0.1, and 1 µL inoculated onto pre-dried LB plates with 0.3 % agar. Cells were incubated at 37 °C statically overnight, with motility determined by measuring the swarming diameter.

Transformation assay

Chitin-induced transformation frequency was measured as described with defined artificial sea water (450 mM NaCl, 10 mM KCl, 9 mM $CaCl_2$, 30 mM $MgCl_2 \cdot 6H_2O$, and 16 mM $MgSO_4 \cdot 7H_2O$; pH 7.8) (57). Bacteria were incubated with extracellular DNA in triplicate wells containing crab shell tabs, and transformation frequency calculated as Spectinomycin resistant ($Spec^r$) CFU ml^{-1} / total CFU ml^{-1}.

QS-dependent Luciferase assay

A previously described pBB1 cosmid was used as a QS-dependent *lux* reporter in *V. cholerae* (58). Overnight cultures of the *V. cholerae* strains were diluted to OD_{600} = 0.001 in liquid LB in microtiter plates and incubated at 37 °C with shaking. The OD_{600} and luminescence were measured each h with a BioTek (VT, USA) Synergy H1 microplate reader to calculate Relative Luminescence Units (RLU) as Luminescence/OD_{600}. *V. cholerae* without the cosmid served as a negative control (no reporter control). Data were collected when OD_{600} = 0.6-0.8. LB medium was used to blank the microplate reader for OD_{600} and luminescence readings.

GFP transcriptional reporter quantification

Overnight cultures of *V. cholerae* or *E. coli* were diluted 1:100 and incubated at 37 °C for 3 h. To enhance the translation of *gfp*, the sequence of the native RBS (12 nt sequence) was

297 replaced with the T7 RBS (12 nt sequence) in the primers used to make the fusions. Cm was
298 added to maintain the plasmid-borne versions of reporters that were cloned into plasmid
299 pSLS3. 300 µL aliquots were transferred to black microtiter plates to read the OD_{600} and GFP
300 fluorescence (Excitation: 485, Emission: 528) with a BioTek Synergy H1 microplate reader (VT,
301 USA) to calculate Relative Fluorescence Units (RFU) as Fluorescence/OD_{600}. LB medium was
302 used as the blank for the OD_{600}. Strain lacking reporters were used to blank the
303 spectrophotometer for GFP fluorescence measurements.
304
305 T6-mediated killing assay
306 Overnight cultures of *V. cholerae* or *E. coli* were back-diluted 1:100 and incubated at 37 °C for
307 3 h. *V. cholerae* strains and the Cm^r *E. coli* target were normalized to OD_{600} = 1 and then mixed
308 at a ratio of either 10:1 or 1:5. A 50 µL mixed culture was spotted onto LB agar and dried. After
309 a 3 h incubation at 37°C, cells were resuspended in 5 ml of LB, and serial dilutions were
310 conducted. Finally, the resuspension was inoculated on a LB agar containing Cm to select for
311 the surviving *E. coli*, which was incubated overnight at 37 °C and the *E. coli* colonies were
312 counted and shown as CFU mL^{-1}.
313
314 RNA extraction and determination of the +1 of transcription by 5'-RACE

315 Overnight cultures of *V. cholerae* were back-diluted 1:100 and incubated at 37 °C for 3 h before
316 lysing. Three independent cultures of T6-active *V. cholerae* C6706 *qstR** and 3223-74 WT were
317 harvested by centrifugation at room temperature. RNA isolation, genomic DNA removal, and
318 RNA clean-up were performed as previously described (59). Genomic DNA contamination was
319 confirmed by conducting PCR with primer pair specific for 16S rRNA loci (*rrsA*) as previously
320 described (Table S3) (60). RNA purity was confirmed by NanoDrop (260 / 280 ≈ 2.0).
321
322 5'-RACE (Invitrogen™ - MA, USA) was conducted according to the manufacturer's protocol
323 with slight modifications. Specifically, SuperScript™ IV reverse transcriptase (Invitrogen™ -
324 MA, USA) was used to complete the first strand cDNA synthesis. Two *vipA*-specific primers
325 (GT3056 and GT3060) were used to identify the +1 of transcription for the major T6 gene
326 cluster (Table S3). PCR products were purified with QIAquick PCR purification kit (Qiagen -
327 Hilden, Germany) or Zymoclean gel DNA recovery kit (Zymo Research - CA, USA). Sanger
328 sequencing was conducted by Eton Bioscience Inc. (NC, USA) with the corresponding nesting
329 primer (Table S3).
330
331 Genomic and phylogenetic analysis
332 Genome sequences of *V. cholerae* strains were collected from NCBI Genome database (Table
333 S4) (61). The IGR upstream of major T6 cluster was extracted, aligned, and presented using

BLAST+ v2.2.18 (62), MUSCLE v3.8 (https://www.ebi.ac.uk/Tools/msa/muscle/) (63, 64), and ESPript 3.0 (https://espript.ibcp.fr/) (38). The DNA sequence of the IGR was used for phylogenetic analysis, and the phylogenetic tree was constructed by the Maximum likelihood method using MEGA11 (65, 66).

For 2012V-1001, 2011EL-1939, 2011EL-1938, and 2011EL-1141 that do not have genome sequence available, colony PCR was conducted to amplify the 5' IGR of the major T6 cluster using OneTaq DNA Polymerase (New England Biolabs – MA, USA). PCR products were confirmed with gel electrophoresis and Sanger sequencing by Eton Bioscience Inc. (NC, USA) with the identical primer pair (Table S3).

Acknowledgements

We would like to thank Dr. Jyl S. Matson for assistance with RNA isolation and Dr. Marvin Whiteley and current and past members of the Hammer Lab for critiques and discussion, specifically, Dr. Samit Watve and Rakin Choudhury for bioinformatic advice and assistance.

Competing interests

The authors have no competing interests.

Uncategorized References

1. Wray GA. The evolutionary significance of cis-regulatory mutations. Nature reviews Genetics. 2007;8(3):206-16. Epub 2007/02/17. doi: 10.1038/nrg2063. PubMed PMID: 17304246.

2. Stern DL, Orgogozo V. THE LOCI OF EVOLUTION: HOW PREDICTABLE IS GENETIC EVOLUTION? Evolution. 2008;62(9):2155-77. doi: https://doi.org/10.1111/j.1558-5646.2008.00450.x.

3. Wittkopp PJ, Kalay G. Cis-regulatory elements: molecular mechanisms and evolutionary processes underlying divergence. Nature reviews Genetics. 2011;13(1):59-69. Epub 2011/12/07. doi: 10.1038/nrg3095. PubMed PMID: 22143240.

4. Norsworthy AN, Visick KL. Signaling between two interacting sensor kinases promotes biofilms and colonization by a bacterial symbiont. Mol Microbiol. 2015;96(2):233-48. Epub 2015/01/15. doi: 10.1111/mmi.12932. PubMed PMID: 25586643; PMCID: PMC4465548.

5. Mandel MJ, Wollenberg MS, Stabb EV, Visick KL, Ruby EG. A single regulatory gene is sufficient to alter bacterial host range. Nature. 2009;458(7235):215-8. Epub 2009/02/03. doi: 10.1038/nature07660. PubMed PMID: 19182778; PMCID: PMC2713604.

6. Perez JC, Groisman EA. Evolution of transcriptional regulatory circuits in bacteria. Cell. 2009;138(2):233-44. Epub 2009/07/28. doi: 10.1016/j.cell.2009.07.002. PubMed PMID: 19632175; PMCID: PMC2726713.

7. Dziejman M, Balon E, Boyd D, Fraser CM, Heidelberg JF, Mekalanos JJ. Comparative genomic analysis of Vibrio cholerae: genes that correlate with cholera endemic and pandemic disease. Proceedings of the National Academy of Sciences of the United States of America. 2002;99(3):1556-61. Epub 2002/01/31. doi: 10.1073/pnas.042667999. PubMed PMID: 11818571; PMCID: PMC122229.

8. Faruque SM, Albert MJ, Mekalanos JJ. Epidemiology, Genetics, and Ecology of ToxigenicVibrio cholerae. Microbiology and Molecular Biology Reviews. 1998;62(4):1301-14. doi: doi:10.1128/MMBR.62.4.1301-1314.1998.

9. Karaolis DKR, Johnson JA, Bailey CC, Boedeker EC, Kaper JB, Reeves PR. A Vibrio cholerae pathogenicity island associated with epidemic and pandemic strains. Proceedings of the National Academy of Sciences. 1998;95(6):3134-9. doi: 10.1073/pnas.95.6.3134.

10. Pruzzo C, Vezzulli L, Colwell RR. Global impact of Vibrio cholerae interactions with chitin. Environ Microbiol. 2008;10(6):1400-10. Epub 2008/03/04. doi: 10.1111/j.1462-2920.2007.01559.x. PubMed PMID: 18312392.

11. Crisan CV, Chande AT, Williams K, Raghuram V, Rishishwar L, Steinbach G, Watve SS, Yunker P, Jordan IK, Hammer BK. Analysis of Vibrio cholerae genomes identifies new type VI secretion system gene clusters. Genome Biol. 2019;20(1):163. Epub 2019/08/14. doi: 10.1186/s13059-019-1765-5. PubMed PMID: 31405375; PMCID: PMC6691524.

12. MacIntyre DL, Miyata ST, Kitaoka M, Pukatzki S. The Vibrio cholerae type VI secretion system displays antimicrobial properties. Proceedings of the National Academy of Sciences of the United States of America. 2010;107(45):19520-4. Epub 2010/10/27. doi: 10.1073/pnas.1012931107. PubMed PMID: 20974937; PMCID: PMC2984155.

13. Gallegos-Monterrosa R, Coulthurst SJ. The ecological impact of a bacterial weapon: microbial interactions and the Type VI secretion system. FEMS Microbiol Rev. 2021;45(6). Epub 2021/06/23. doi: 10.1093/femsre/fuab033. PubMed PMID: 34156081; PMCID: PMC8632748.

14. Hussain NAS, Kirchberger PC, Case RJ, Boucher YF. Modular Molecular Weaponry Plays a Key Role in Competition Within an Environmental Vibrio cholerae Population. Frontiers in Microbiology. 2021;12(979). doi: 10.3389/fmicb.2021.671092.

15. Ishikawa T, Sabharwal D, Bröms J, Milton DL, Sjöstedt A, Uhlin BE, Wai SN, Camilli A. Pathoadaptive Conditional Regulation of the Type VI Secretion System in Vibrio cholerae O1 Strains. Infection and Immunity. 2012;80(2):575-84. doi: doi:10.1128/IAI.05510-11.

16. Kirchberger PC, Unterweger D, Provenzano D, Pukatzki S, Boucher Y. Sequential displacement of Type VI Secretion System effector genes leads to evolution of diverse immunity gene arrays in Vibrio cholerae. Scientific Reports. 2017;7(1):45133. doi: 10.1038/srep45133.

17. Santoriello FJ, Pukatzki S. When the pandemic opts for the lockdown: Secretion system evolution in the cholera bacterium. Microb Cell. 2021;8(3):69-72. Epub 2021/03/09. doi:

409 10.15698/mic2021.03.744. PubMed PMID: 33681340; PMCID: PMC7919388.

410 18. Unterweger D, Miyata ST, Bachmann V, Brooks TM, Mullins T, Kostiuk B, Provenzano D,

411 Pukatzki S. The Vibrio cholerae type VI secretion system employs diverse effector modules for

412 intraspecific competition. Nature Communications. 2014;5(1):3549. doi:

413 10.1038/ncomms4549.

414 19. Kostiuk B, Santoriello FJ, Diaz-Satizabal L, Bisaro F, Lee K-J, Dhody AN, Provenzano D,

415 Unterweger D, Pukatzki S. Type VI secretion system mutations reduced competitive fitness of

416 classical Vibrio cholerae biotype. Nature Communications. 2021;12(1):6457. doi:

417 10.1038/s41467-021-26847-y.

418 20. Crisan CV, Chandrashekar H, Everly C, Steinbach G, Hill SE, Yunker PJ, Lieberman RR,

419 Hammer BK, Ellermeier CD. A New Contact Killing Toxin Permeabilizes Cells and Belongs to a

420 Broadly Distributed Protein Family. mSphere. 2021;6(4):e00318-21. doi:

421 doi:10.1128/mSphere.00318-21.

422 21. Drebes Dörr NC, Blokesch M. Interbacterial competition and anti-predatory behaviour of

423 environmental Vibrio cholerae strains. Environmental Microbiology. 2020;22(10):4485-504.

424 doi: https://doi.org/10.1111/1462-2920.15224.

425 22. Crisan CV, Hammer BK. The Vibrio cholerae type VI secretion system: toxins, regulators

426 and consequences. Environ Microbiol. 2020;22(10):4112-22. Epub 2020/03/07. doi:

427 10.1111/1462-2920.14976. PubMed PMID: 32133757.

428 23. Jaskolska M, Stutzmann S, Stoudmann C, Blokesch M. QstR-dependent regulation of
429 natural competence and type VI secretion in Vibrio cholerae. Nucleic Acids Res.
430 2018;46(20):10619-34. Epub 2018/08/14. doi: 10.1093/nar/gky717. PubMed PMID:
431 30102403; PMCID: PMC6237807.
432 24. Joshi A, Kostiuk B, Rogers A, Teschler J, Pukatzki S, Yildiz FH. Rules of Engagement: The
433 Type VI Secretion System in Vibrio cholerae. Trends Microbiol. 2017;25(4):267-79. Epub
434 2016/12/29. doi: 10.1016/j.tim.2016.12.003. PubMed PMID: 28027803; PMCID:
435 PMC5365375.
436 25. Joshi A, Mahmoud SA, Kim SK, Ogdahl JL, Lee VT, Chien P, Yildiz FH. c-di-GMP inhibits
437 LonA-dependent proteolysis of TfoY in Vibrio cholerae. PLoS Genet. 2020;16(6):e1008897.
438 Epub 2020/06/27. doi: 10.1371/journal.pgen.1008897. PubMed PMID: 32589664; PMCID:
439 PMC7371385.
440 26. Metzger LC, Stutzmann S, Scrignari T, Van der Henst C, Matthey N, Blokesch M.
441 Independent Regulation of Type VI Secretion in Vibrio cholerae by TfoX and TfoY. Cell Rep.
442 2016;15(5):951-8. Epub 2016/04/28. doi: 10.1016/j.celrep.2016.03.092. PubMed PMID:
443 27117415; PMCID: PMC4858559.
444 27. Lo Scrudato M, Blokesch M. A transcriptional regulator linking quorum sensing and chitin
445 induction to render Vibrio cholerae naturally transformable. Nucleic Acids Res.
446 2013;41(6):3644-58. Epub 2013/02/06. doi: 10.1093/nar/gkt041. PubMed PMID: 23382174;

447 PMCID: PMC3616704.

448 28. Meibom KL, Blokesch M, Dolganov NA, Wu CY, Schoolnik GK. Chitin induces natural
449 competence in Vibrio cholerae. Science. 2005;310(5755):1824-7. Epub 2005/12/17. doi:
450 10.1126/science.1120096. PubMed PMID: 16357262.

451 29. Watve SS, Thomas J, Hammer BK. CytR Is a Global Positive Regulator of Competence,
452 Type VI Secretion, and Chitinases in Vibrio cholerae. PLoS One. 2015;10(9):e0138834. Epub
453 2015/09/25. doi: 10.1371/journal.pone.0138834. PubMed PMID: 26401962; PMCID:
454 PMC4581735.

455 30. Tsou AM, Cai T, Liu Z, Zhu J, Kulkarni RV. Regulatory targets of quorum sensing in Vibrio
456 cholerae: evidence for two distinct HapR-binding motifs. Nucleic Acids Res. 2009;37(8):2747-
457 56. Epub 2009/03/12. doi: 10.1093/nar/gkp121. PubMed PMID: 19276207; PMCID:
458 PMC2677876.

459 31. Bernardy EE, Turnsek MA, Wilson SK, Tarr CL, Hammer BK, Liu S-J. Diversity of Clinical and
460 Environmental Isolates of Vibrio cholerae in Natural Transformation and Contact-Dependent
461 Bacterial Killing Indicative of Type VI Secretion System Activity. Applied and Environmental
462 Microbiology. 2016;82(9):2833-42. doi: doi:10.1128/AEM.00351-16.

463 32. Dunn JJ, Studier FW. Complete nucleotide sequence of bacteriophage T7 DNA and the
464 locations of T7 genetic elements. J Mol Biol. 1983;166(4):477-535. Epub 1983/06/05. doi:
465 10.1016/s0022-2836(83)80282-4. PubMed PMID: 6864790.

33. Jobling MG, Holmes RK. Characterization of hapR, a positive regulator of the Vibrio cholerae HA/protease gene hap, and its identification as a functional homologue of the Vibrio harveyi luxR gene. Molecular Microbiology. 1997;26(5):1023-34. doi: https://doi.org/10.1046/j.1365-2958.1997.6402011.x.

34. Pursley BR, Maiden MM, Hsieh ML, Fernandez NL, Severin GB, Waters CM. Cyclic di-GMP Regulates TfoY in Vibrio cholerae To Control Motility by both Transcriptional and Posttranscriptional Mechanisms. J Bacteriol. 2018;200(7). Epub 2018/01/10. doi: 10.1128/JB.00578-17. PubMed PMID: 29311281; PMCID: PMC5847662.

35. Schneider CA, Rasband WS, Eliceiri KW. NIH Image to ImageJ: 25 years of image analysis. Nat Methods. 2012;9(7):671-5. Epub 2012/08/30. doi: 10.1038/nmeth.2089. PubMed PMID: 22930834; PMCID: PMC5554542.

36. Zheng J, Shin OS, Cameron DE, Mekalanos JJ. Quorum sensing and a global regulator TsrA control expression of type VI secretion and virulence in Vibrio cholerae. Proceedings of the National Academy of Sciences. 2010;107(49):21128-33. doi: 10.1073/pnas.1014998107.

37. Joelsson A, Liu Z, Zhu J. Genetic and phenotypic diversity of quorum-sensing systems in clinical and environmental isolates of Vibrio cholerae. Infect Immun. 2006;74(2):1141-7. Epub 2006/01/24. doi: 10.1128/IAI.74.2.1141-1147.2006. PubMed PMID: 16428762; PMCID: PMC1360356.

485 38. Robert X, Gouet P. Deciphering key features in protein structures with the new ENDscript
486 server. Nucleic Acids Res. 2014;42(Web Server issue):W320-4. Epub 2014/04/23. doi:
487 10.1093/nar/gku316. PubMed PMID: 24753421; PMCID: PMC4086106.
488 39. Holowka J, Zakrzewska-Czerwinska J. Nucleoid Associated Proteins: The Small Organizers
489 That Help to Cope With Stress. Front Microbiol. 2020;11:590. Epub 2020/05/07. doi:
490 10.3389/fmicb.2020.00590. PubMed PMID: 32373086; PMCID: PMC7177045.
491 40. Ayala JC, Silva AJ, Benitez JA. H-NS: an overarching regulator of the Vibrio cholerae life
492 cycle. Res Microbiol. 2017;168(1):16-25. Epub 2016/08/06. doi:
493 10.1016/j.resmic.2016.07.007. PubMed PMID: 27492955; PMCID: PMC5241179.
494 41. Chaparian RR, Olney SG, Hustmyer CM, Rowe-Magnus DA, van Kessel JC. Integration host
495 factor and LuxR synergistically bind DNA to coactivate quorum-sensing genes in Vibrio harveyi.
496 Mol Microbiol. 2016;101(5):823-40. Epub 2016/05/19. doi: 10.1111/mmi.13425. PubMed
497 PMID: 27191515.
498 42. Papenfort K, Forstner KU, Cong JP, Sharma CM, Bassler BL. Differential RNA-seq of Vibrio
499 cholerae identifies the VqmR small RNA as a regulator of biofilm formation. Proceedings of
500 the National Academy of Sciences of the United States of America. 2015;112(7):E766-75. Epub
501 2015/02/04. doi: 10.1073/pnas.1500203112. PubMed PMID: 25646441; PMCID:
502 PMC4343088.
503 43. Shao Y, Bassler BL. Quorum regulatory small RNAs repress type VI secretion in Vibrio

cholerae. Mol Microbiol. 2014;92(5):921-30. Epub 2014/04/05. doi: 10.1111/mmi.12599. PubMed PMID: 24698180; PMCID: PMC4038675.

44. Drebes Dorr NC, Proutiere A, Jaskolska M, Stutzmann S, Bader L, Blokesch M. Single nucleotide polymorphism determines constitutive versus inducible type VI secretion in Vibrio cholerae. ISME J. 2022. Epub 2022/04/13. doi: 10.1038/s41396-022-01234-7. PubMed PMID: 35411099.

45. Gourse RL, Ross W, Gaal T. UPs and downs in bacterial transcription initiation: the role of the alpha subunit of RNA polymerase in promoter recognition. Mol Microbiol. 2000;37(4):687-95. Epub 2000/09/06. doi: 10.1046/j.1365-2958.2000.01972.x. PubMed PMID: 10972792.

46. Guo C, McDowell IC, Nodzenski M, Scholtens DM, Allen AS, Lowe WL, Reddy TE. Transversions have larger regulatory effects than transitions. BMC Genomics. 2017;18(1):394. doi: 10.1186/s12864-017-3785-4.

47. Slattery M, Zhou T, Yang L, Dantas Machado AC, Gordân R, Rohs R. Absence of a simple code: how transcription factors read the genome. Trends in Biochemical Sciences. 2014;39(9):381-99. doi: 10.1016/j.tibs.2014.07.002.

48. MacKenzie KD, Wang Y, Musicha P, Hansen EG, Palmer MB, Herman DJ, Feasey NA, White AP. Parallel evolution leading to impaired biofilm formation in invasive Salmonella strains. PLoS Genet. 2019;15(6):e1008233. Epub 2019/06/25. doi: 10.1371/journal.pgen.1008233.

523 PubMed PMID: 31233504; PMCID: PMC6611641.

524 49. Osborne SE, Walthers D, Tomljenovic AM, Mulder DT, Silphaduang U, Duong N, Lowden
525 MJ, Wickham ME, Waller RF, Kenney LJ, Coombes BK. Pathogenic adaptation of intracellular
526 bacteria by rewiring a cis-regulatory input function. Proceedings of the National
527 Academy of Sciences. 2009;106(10):3982-7. doi: 10.1073/pnas.0811669106.

528 50. Unterweger D, Kitaoka M, Miyata ST, Bachmann V, Brooks TM, Moloney J, Sosa O, Silva D,
529 Duran-Gonzalez J, Provenzano D, Pukatzki S. Constitutive type VI secretion system expression
530 gives Vibrio cholerae intra- and interspecific competitive advantages. PLoS One.
531 2012;7(10):e48320. Epub 2012/10/31. doi: 10.1371/journal.pone.0048320. PubMed PMID:
532 23110230; PMCID: PMC3482179.

533 51. Fu Y, Waldor MK, Mekalanos JJ. Tn-Seq analysis of Vibrio cholerae intestinal colonization
534 reveals a role for T6SS-mediated antibacterial activity in the host. Cell Host Microbe.
535 2013;14(6):652-63. Epub 2013/12/18. doi: 10.1016/j.chom.2013.11.001. PubMed PMID:
536 24331463; PMCID: PMC3951154.

537 52. Zhao W, Caro F, Robins W, Mekalanos JJ. Antagonism toward the intestinal microbiota
538 and its effect on Vibrio cholerae virulence. Science. 2018;359(6372):210-3. Epub 2018/01/13.
539 doi: 10.1126/science.aap8775. PubMed PMID: 29326272; PMCID: PMC8010019.

540 53. Logan SL, Thomas J, Yan J, Baker RP, Shields DS, Xavier JB, Hammer BK, Parthasarathy R.
541 The Vibrio cholerae type VI secretion system can modulate host intestinal

542 mechanics to displace gut bacterial symbionts. Proceedings of the National Academy of
543 Sciences. 2018;115(16):E3779-E87. doi: 10.1073/pnas.1720133115.
544 54. Seal S, Dharmarajan G, Khan I. Evolution of pathogen tolerance and emerging infections:
545 A missing experimental paradigm. Elife. 2021;10. Epub 2021/09/22. doi: 10.7554/eLife.68874.
546 PubMed PMID: 34544548; PMCID: PMC8455132.
547 55. San JE, Baichoo S, Kanzi A, Moosa Y, Lessells R, Fonseca V, Mogaka J, Power R, de Oliveira
548 T. Current Affairs of Microbial Genome-Wide Association Studies: Approaches, Bottlenecks
549 and Analytical Pitfalls. Front Microbiol. 2019;10:3119. Epub 2020/02/23. doi:
550 10.3389/fmicb.2019.03119. PubMed PMID: 32082269; PMCID: PMC7002396.
551 56. Skorupski K, Taylor RK. Positive selection vectors for allelic exchange. Gene.
552 1996;169(1):47-52. Epub 1996/02/22. doi: 10.1016/0378-1119(95)00793-8. PubMed PMID:
553 8635748.
554 57. Watve SS, Bernardy EE, Hammer BK. Vibrio cholerae: Measuring Natural Transformation
555 Frequency. Curr Protoc Microbiol. 2014;35:6A 4 1-12. Epub 2014/11/05. doi:
556 10.1002/9780471729259.mc06a04s35. PubMed PMID: 25367272.
557 58. Miller MB, Skorupski K, Lenz DH, Taylor RK, Bassler BL. Parallel quorum sensing systems
558 converge to regulate virulence in Vibrio cholerae. Cell. 2002;110(3):303-14. Epub 2002/08/15.
559 doi: 10.1016/s0092-8674(02)00829-2. PubMed PMID: 12176318.
560 59. Matson JS. Preparation of Vibrio cholerae Samples for RNA-seq Analysis. Methods Mol

561 Biol. 2018;1839:29-38. Epub 2018/07/27. doi: 10.1007/978-1-4939-8685-9_3. PubMed PMID:
562 30047051.
563 60. Manera K, Caro F, Li H, Pei TT, Hersch SJ, Mekalanos JJ, Dong TG. Sensing of intracellular
564 Hcp levels controls T6SS expression in Vibrio cholerae. Proceedings of the National Academy
565 of Sciences of the United States of America. 2021;118(25). Epub 2021/06/24. doi:
566 10.1073/pnas.2104813118. PubMed PMID: 34161288; PMCID: PMC8237632.
567 61. Sayers EW, Agarwala R, Bolton EE, Brister JR, Canese K, Clark K, Connor R, Fiorini N, Funk
568 K, Hefferon T, Holmes JB, Kim S, Kimchi A, Kitts PA, Lathrop S, Lu Z, Madden TL, Marchler-Bauer
569 A, Phan L, Schneider VA, Schoch CL, Pruitt KD, Ostell J. Database resources of the National
570 Center for Biotechnology Information. Nucleic Acids Res. 2019;47(D1):D23-D8. Epub
571 2018/11/06. doi: 10.1093/nar/gky1069. PubMed PMID: 30395293; PMCID: PMC6323993.
572 62. Camacho C, Coulouris G, Avagyan V, Ma N, Papadopoulos J, Bealer K, Madden TL. BLAST+:
573 architecture and applications. BMC Bioinformatics. 2009;10:421. Epub 2009/12/17. doi:
574 10.1186/1471-2105-10-421. PubMed PMID: 20003500; PMCID: PMC2803857.
575 63. Edgar RC. MUSCLE: multiple sequence alignment with high accuracy and high throughput.
576 Nucleic Acids Res. 2004;32(5):1792-7. Epub 2004/03/23. doi: 10.1093/nar/gkh340. PubMed
577 PMID: 15034147; PMCID: PMC390337.
578 64. Madeira F, Park YM, Lee J, Buso N, Gur T, Madhusoodanan N, Basutkar P, Tivey ARN,
579 Potter SC, Finn RD, Lopez R. The EMBL-EBI search and sequence analysis tools APIs in 2019.

Nucleic Acids Res. 2019;47(W1):W636-W41. Epub 2019/04/13. doi: 10.1093/nar/gkz268. PubMed PMID: 30976793; PMCID: PMC6602479.

65. Felsenstein J. Evolutionary trees from DNA sequences: a maximum likelihood approach. J Mol Evol. 1981;17(6):368-76. Epub 1981/01/01. doi: 10.1007/BF01734359. PubMed PMID: 7288891.

66. Tamura K, Stecher G, Kumar S. MEGA11: Molecular Evolutionary Genetics Analysis Version 11. Mol Biol Evol. 2021;38(7):3022-7. Epub 2021/04/24. doi: 10.1093/molbev/msab120. PubMed PMID: 33892491; PMCID: PMC8233496.

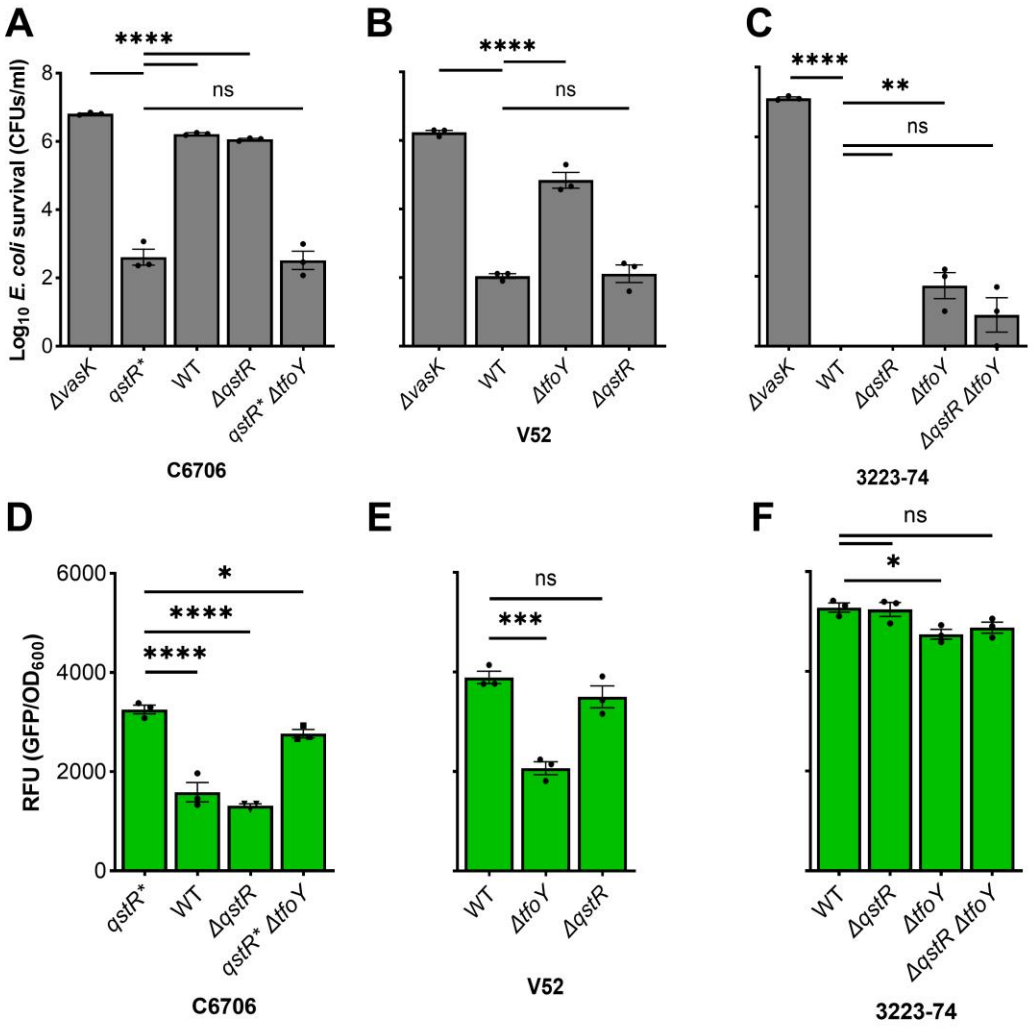
A
B
C
D
E
F
G
Log10 E. coli survival (CFUs/ml)
RFU (GFP/OD600)
****
ns
**
***
*
ΔvasK
qstR*
WT
ΔqstR
qstR* ΔtfoY
ΔtfoY
ΔqstR ΔtfoY
C6706
V52
3223-74
3223-74 ΔvasK
3223-74
3223-74 ΔtfoY
0 h
3 h

589

Figure 1. *Vibrio cholerae* 3223-74 T6 activity is QstR- and TfoY-independent. (A-C) *V. cholerae* strains with the indicated genotypes were co-cultured with chloramphenicol resistant (Cm^r) *E. coli* followed by determination of *E. coli* survival by counting of colony forming units (CFUs) on LB agar with Cm. A *V. cholerae ΔvasK* mutant defective in T6 assembly served as a $T6^-$ negative control. (D-F) Relative Fluorescence Units are from reporters with *gfp* fused to the intergenic region 5' of *vipA* derived from the strains shown. The mean value ± S.E. from co-cultures (A-C) and monocultures (D-F) are derived from 3 independent biological replicates. A one-way ANOVA with Dunnett post-hoc test was conducted to determine the significance: ns denotes not significant, ****$p \leq 0.0001$, ***$p \leq 0.001$, **$p \leq 0.01$, *$p \leq 0.05$. (G) *E. coli* cells expressing constitutive *gfp* were competed against 3223-74, with the same frame imaged at 0 h and 3 h by confocal microscopy. In the images, *gfp* signal from the *E. coli* is overlaid on top of bright-light images of the co-culture. Scale bar = 50 µm.

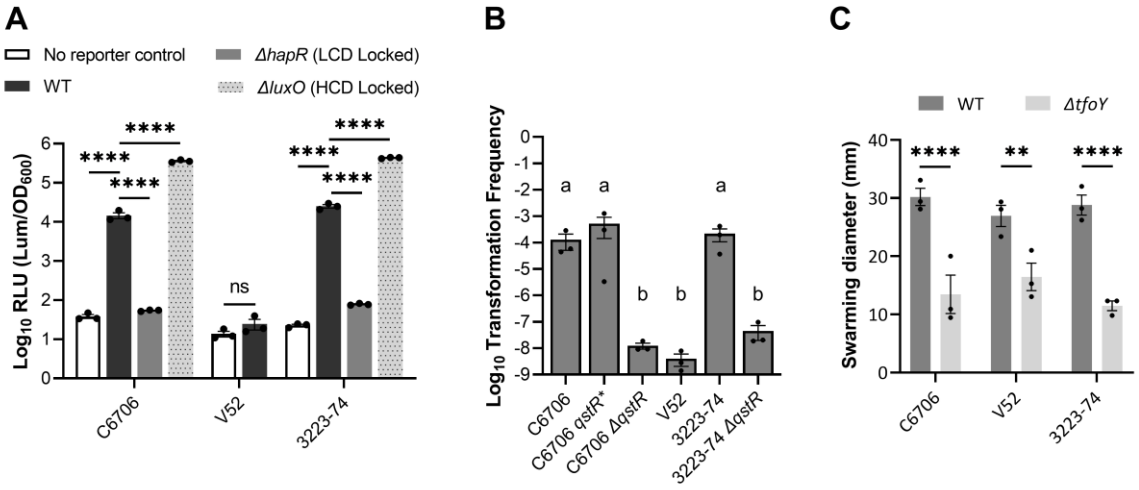

Figure 2. *Vibrio cholerae* 3223-74 encodes functional HapR, QstR, and TfoY. (A) *V. cholerae* strains with and without a QS-dependent *lux* reporter cosmid (pBB1) were grown in liquid LB with relative luminescence units per OD_{600} measured at HCD (OD_{600} = 0.6-0.8). Statistical analyses were conducted with one-way ANOVA with Tukey post-hoc test (C6706 and 3223-74) and one-tailed student's t-test (V52). The *ΔhapR* mutant is defective at QS and effectively "locked" at low cell density, while the *ΔluxO* mutant that constitutively produces HapR is effectively "locked" at high cell density. (B) *V. cholerae* strains with the indicated genotypes were grown in ASW with crab shell and exogenous Spec-marked genomic DNA. Transformation frequency = $Spec^r$ CFU ml^{-1} / total CFU ml^{-1}. Statistical analyses were conducted with one-way ANOVA with Tukey post-hoc test. Letters "a" and "b" identify statistically significance ($p \leq 0.05$) of transformation frequency between *V. cholerae* strains. (C) *V. cholerae* strains were inoculated on 0.3% LB agar and grew overnight. Statistical analyses

were conducted with one-tailed student's t-test. Colony diameters were physically measured from the furthest edges. All data shown are the mean ± S.E. from 3 independent biological replicates. ns: not significant, ****$p \leq 0.0001$, **$p \leq 0.01$.

620

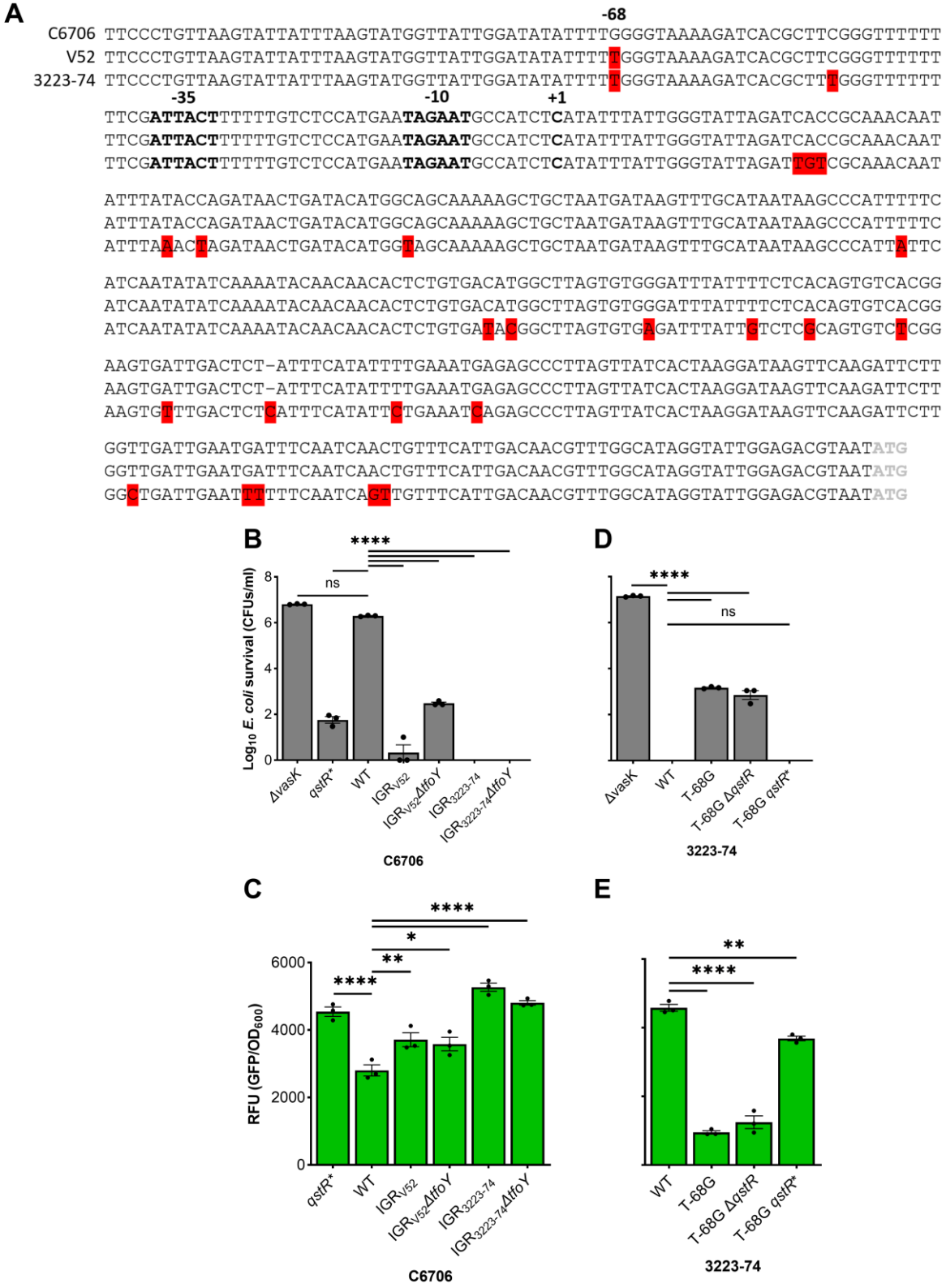
A
-68
C6706 TTCCCTGTTAAGTATTATTTAAGTATGGTTATTGGATATATTTTGGGGTAAAAGATCACGCTTCGGGTTTTTT
V52 TTCCCTGTTAAGTATTATTTAAGTATGGTTATTGGATATATTTTTGGGTAAAAGATCACGCTTCGGGTTTTTT
3223-74 TTCCCTGTTAAGTATTATTTAAGTATGGTTATTGGATATATTTTTGGGTAAAAGATCACGCTTTGGGTTTTTT
-35
-10
+1
TTCGATTACTTTTTTGTCTCCATGAATAGAATGCCATCTCATATTTATTGGGTATTAGATCACCGCAAACAAT
TTCGATTACTTTTTTGTCTCCATGAATAGAATGCCATCTCATATTTATTGGGTATTAGATCACCGCAAACAAT
TTCGATTACTTTTTTGTCTCCATGAATAGAATGCCATCTCATATTTATTGGGTATTAGATTGTCGCAAACAAT
ATTTATACCAGATAACTGATACATGGCAGCAAAAAGCTGCTAATGATAAGTTTGCATAATAAGCCCATTTTTC
ATTTATACCAGATAACTGATACATGGCAGCAAAAAGCTGCTAATGATAAGTTTGCATAATAAGCCCATTTTTC
ATTTAAACTAGATAACTGATACATGGTAGCAAAAAGCTGCTAATGATAAGTTTGCATAATAAGCCCATTATTC
ATCAATATATCAAAATACAACAACACTCTGTGACATGGCTTAGTGTGGGATTTATTTTCTCACAGTGTCACGG
ATCAATATATCAAAATACAACAACACTCTGTGACATGGCTTAGTGTGGGATTTATTTTCTCACAGTGTCACGG
ATCAATATATCAAAATACAACAACACTCTGTGATTACGGCTTAGTGTGAGATTTATTGTCTCGCAGTGTCTCGG
AAGTGATTGACTCT-ATTTCATATTTTGAAATGAGAGCCCTTAGTTATCACTAAGGATAAGTTCAAGATTCTT
AAGTGATTGACTCT-ATTTCATATTTTGAAATGAGAGCCCTTAGTTATCACTAAGGATAAGTTCAAGATTCTT
AAGTGTTTGACTCTCATTTCATATTCTGAAATCAGAGCCCTTAGTTATCACTAAGGATAAGTTCAAGATTCTT
GGTTGATTGAATGATTTCAATCAACTGTTTCATTGACAACGTTTGGCATAGGTATTGGAGACGTAATATG
GGTTGATTGAATGATTTCAATCAACTGTTTCATTGACAACGTTTGGCATAGGTATTGGAGACGTAATATG
GGCTGATTGAATTTTTTCAATCAGTTGTTTCATTGACAACGTTTGGCATAGGTATTGGAGACGTAATATG
B
****
ns
Log10 E. coli survival (CFUs/ml)
8
6
4
2
0
ΔvasK
qstR*
WT
IGRV52
IGRV52ΔtfoY
IGR3223-74
IGR3223-74ΔtfoY
C6706
D
****
ns
ΔvasK
WT
T-68G
T-68G ΔqstR
T-68G qstR*
3223-74
C
****
*
**
****
RFU (GFP/OD600)
6000
4000
2000
0
qstR*
WT
IGRV52
IGRV52ΔtfoY
IGR3223-74
IGR3223-74ΔtfoY
C6706
E
**
****
WT
T-68G
T-68G ΔqstR
T-68G qstR*
3223-74

621

Figure 3. G-68T mutation abolishes QstR dependence in C6706 and T-68G confers QstR dependence to 3223-74. (A) Alignment of the IGR upstream of *vipA* was conducted using MUSCLE. SNPs and MNPs are highlighted in red, one gap indicated with a "–", the putative promoter and the transcriptional start site (TSS; +1) in bold, and the start codon of *vipA* in grey. (B) the C6706 5' IGR of *vipA* was replaced with the IGR from either V52 or 3223-74. (D) A T-68G mutation in the 5' IGR of *vipA* was introduced into 3223-74 with different *qstR* alleles. Competition assays were conducted by co-culturing *V. cholerae* killers and Cm^r *E. coli* target followed by determination of *E. coli* survival by counting of colony forming units (CFUs) on LB agar with Cm. The *V. cholerae ΔvasK* mutant unable to assemble a functional T6 served as a $T6^-$ negative control. (C, E) Shown are fluorescence levels of transcriptional reporters with *gfp* fused to corresponding IGRs of *vipA* expressed in either C6706 (C) or 3223-74 (E). Shown are mean values ± S.E. from 3 independent biological replicates of co-cultures (B and D) and monocultures (C and E). A one-way ANOVA with Dunnett post-hoc test was conducted to determine the significance - ns: not significant, ****$p \leq 0.0001$, **$p \leq 0.01$, *$p \leq 0.05$.

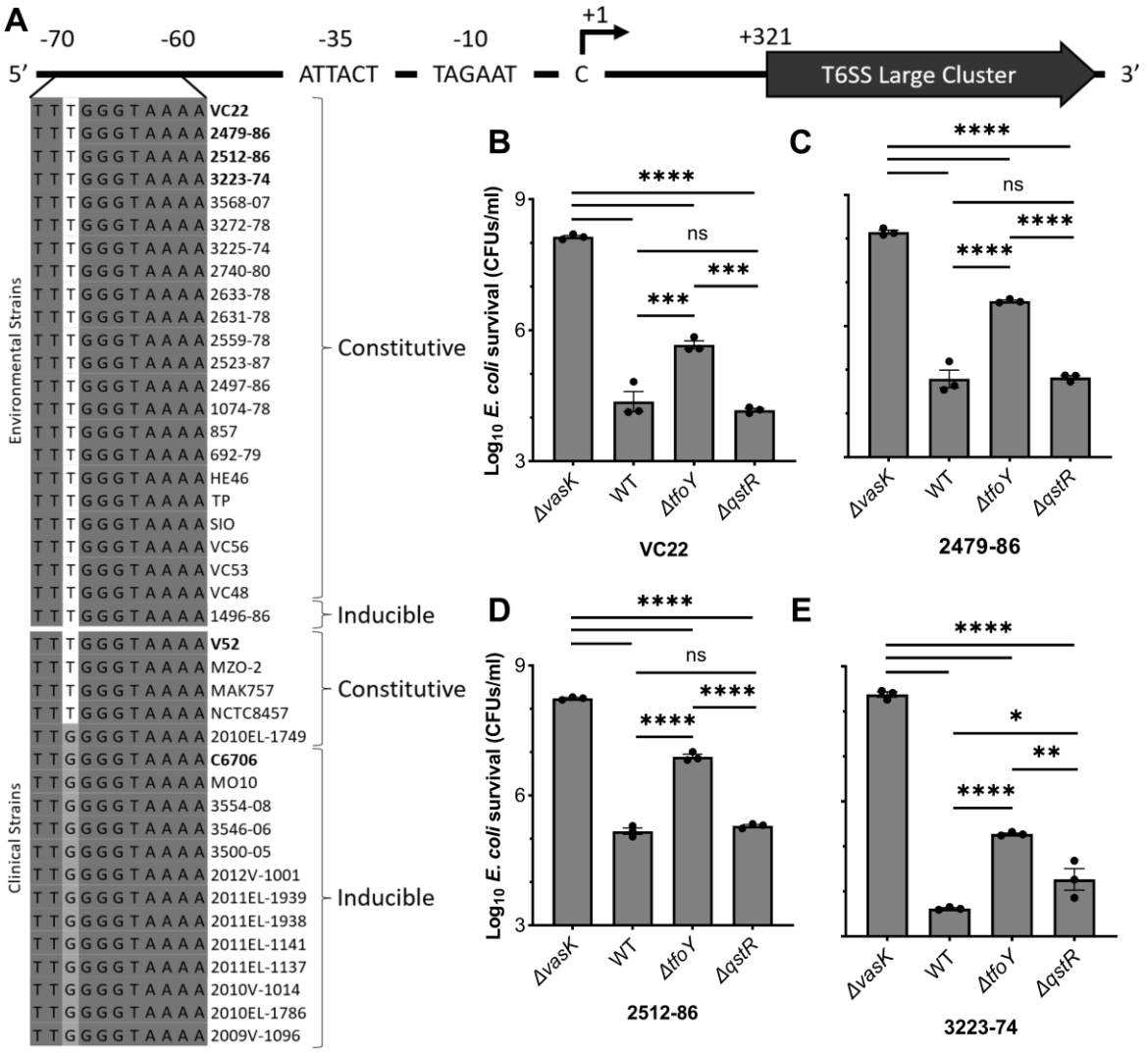

Figure 4. Environmental *V. cholerae* isolates encode a T at position -68 while human, chitin-induced isolates encode a G. (A) A SNP at position -68 in the IGR of the major T6 cluster controls killing activity. Conserved nts are in dark grey and the SNP of interest is highlighted in white/grey. T6 control was categorized as described (31). (B-E) Survival of *E. coli* following competition assays with WT *V. cholerae* strains and mutants was determined by CFU counts. The V. cholerae *ΔvasK* mutant served as a $T6^-$ negative control. Data shown are mean values ± S.E. of 3 independent biological replicates. A one-way ANOVA with Tukey post-hoc test was

644 conducted to determine the significance - ns: not significant, ****p ≤ 0.0001, ***p ≤ 0.001,

645 **p ≤ 0.01, *p ≤ 0.05.

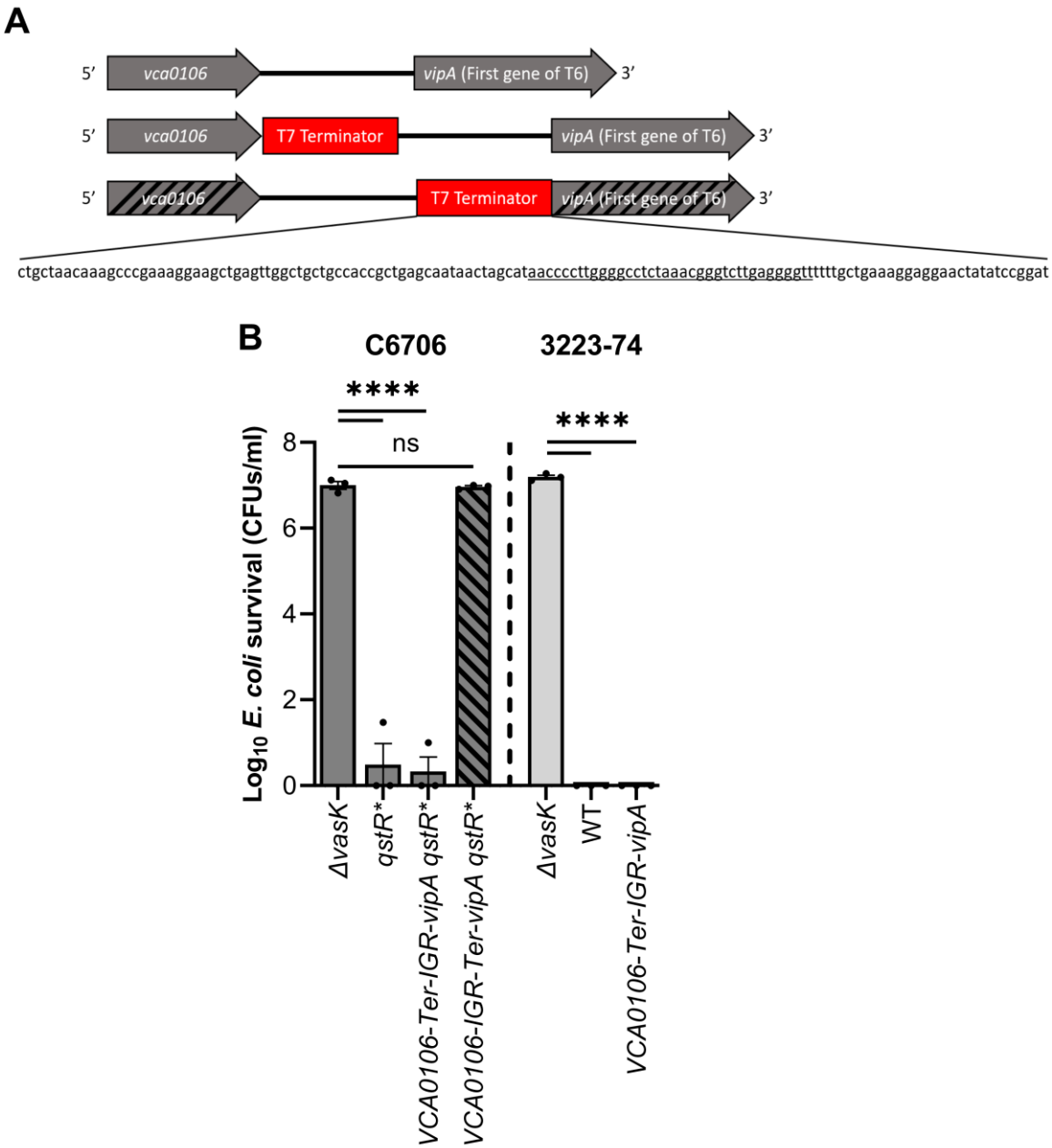

646

647 **Figure S1. Activity of the major T6 gene cluster is not controlled by transcriptional read-**

648 **through.** (A) Schematic shows the wildtype T6 5’ IGR and the DNA sequence and location of

649 the T7 terminator inserted before and after the T6 5’ IGR. The region encoding an RNA hairpin

650 is underlined (32). (B) Competition assays were conducted by co-culturing *V. cholerae* and Cm^r

651 *E. coli* target followed by determination of *E. coli* survival by counting of colony forming units

652 (CFUs) on LB agar with Cm. The *V. cholerae ΔvasK* mutant served as a $T6^-$ negative control.

653 Data shown are mean values ± S.E. from 3 independent biological replicates. A one-way

654 ANOVA with Dunnett post-hoc test was conducted to determine the significance - ns: not

655 significant, ****$p \leq 0.0001$, ns > 0.05.

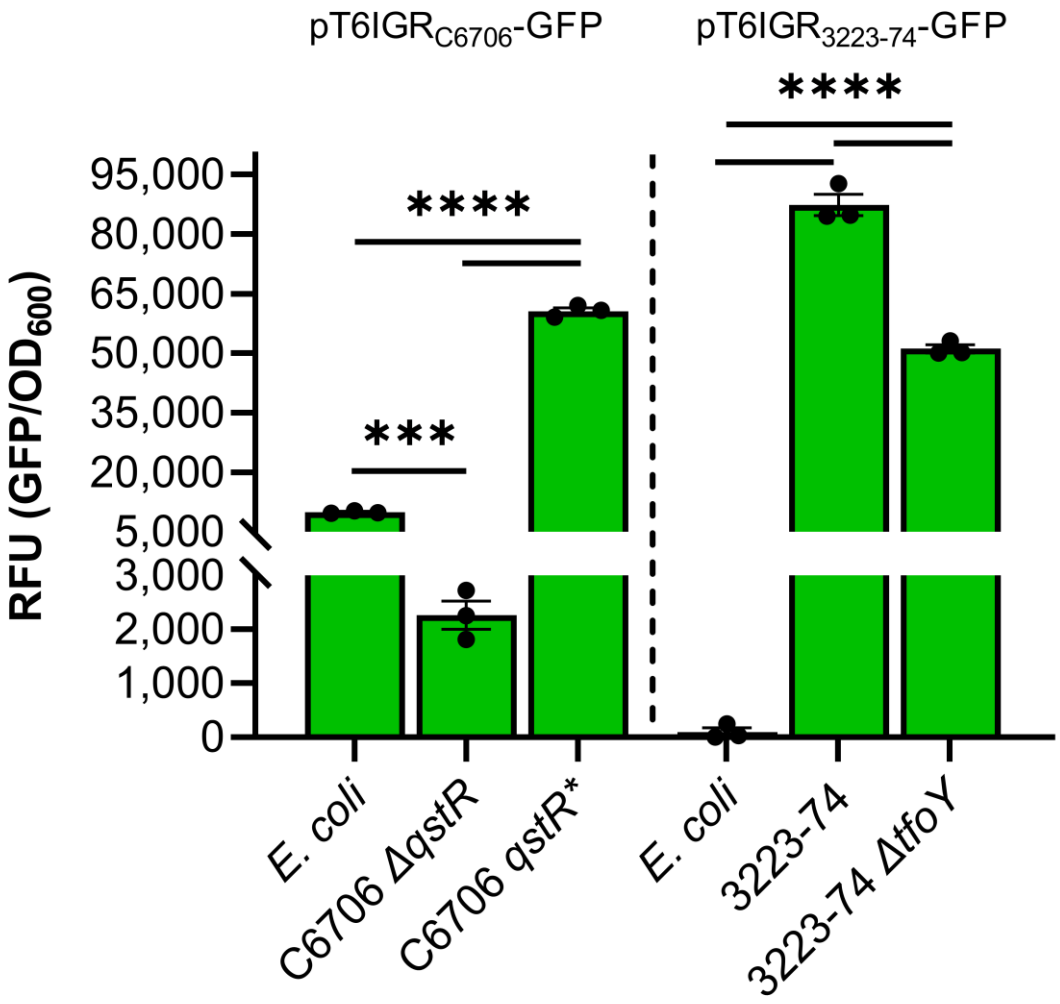

Figure S2. The major *V. cholerae* T6 promoter is not constitutively expressed in *E. coli*. *V. cholerae* or *E. coli* carrying a plasmid-encoded *gfp* gene driven by either the C6706 or 3223-74 5' T6 IGR was grown in liquid LB with Cm. *gfp* is represented as relative fluorescent units per OD_{600} (RFU). Data shown are mean values ± S.E. from 3 independent biological replicates. A one-way ANOVA with Tukey post-hoc test was conducted to determine the significance: ****$p \leq 0.0001$, ***$p \leq 0.001$.

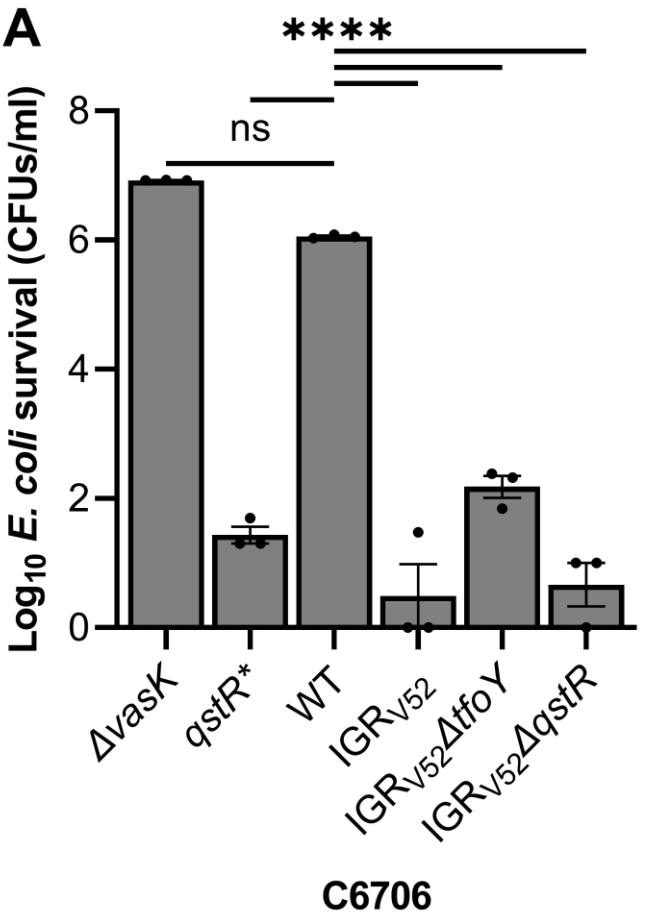
A
****
ns
8
6
4
2
0
Log10 E. coli survival (CFUs/ml)
ΔvasK
qstR*
WT
IGRV52
IGRV52ΔtfoY
IGRV52ΔqstR
C6706

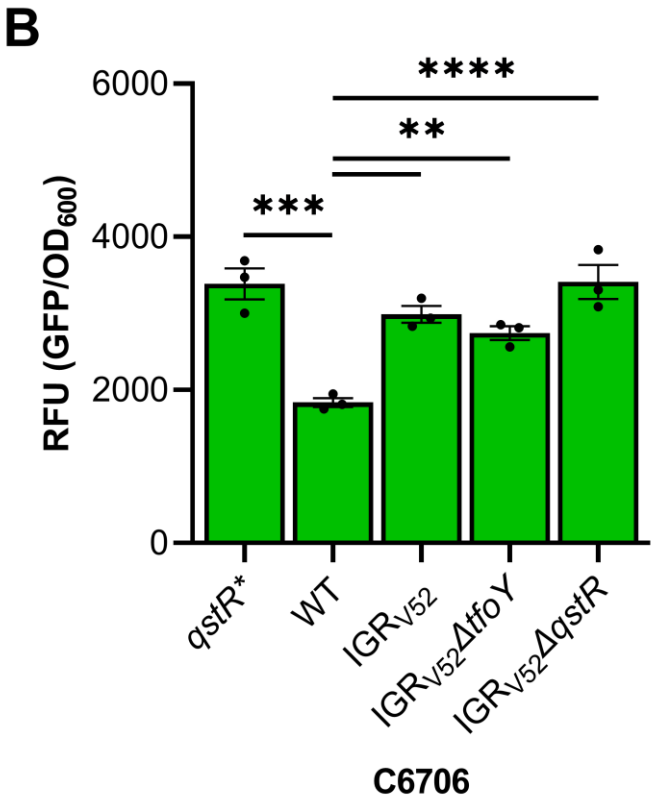
B
****
**
***
6000
4000
2000
0
RFU (GFP/OD600)
qstR*
WT
IGRV52
IGRV52ΔtfoY
IGRV52ΔqstR
C6706

663

Figure S3. C6706 T6 is no longer activated by QstR after acquiring the G-68T mutation. (A) Competition assays were conducted by co-culturing *V. cholerae* and Cm^r *E. coli* target cells followed by determination of *E. coli* survival by counting of colony forming units (CFUs) on LB agar with Cm. The *V. cholerae ΔvasK* mutant served as a $T6^-$ negative control. (B) Fluorescence levels are from reporters with *gfp* fused to the intergenic region 5' of *vipA* derived from the strains shown. Data shown are mean values ± S.E. from 3 independent biological replicates. A one-way ANOVA with Dunnett post-hoc test was conducted to determine the significance - ns: not significant, ****$p \leq 0.0001$, ***$p \leq 0.001$, **$p \leq 0.01$, ns > 0.05.

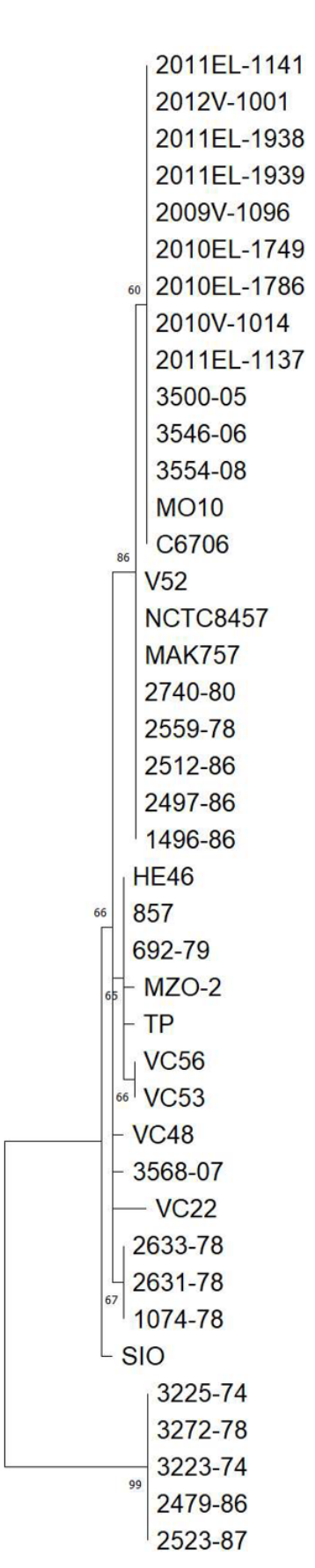

Human/Environmental isolates	nt	Serogroup
H	G	O1
H	G	O1
H	G	O1
H	G	O1
H	G	O1
H	G	O1
H	G	O1
H	G	O1
H	G	O1
H	G	O1
H	G	O1
H	G	O1
H	G	O139
H	G	O1
H	T	O37
H	T	O1
H	T	O1
E	T	O1
E	T	O1
E	T	O1
E	T	O1
E	T	O1
E	T	NAg
E	T	O1
E	T	O1
H	T	O14
E	T	NAg
E	T	O1
E	T	NAg
E	T	NAg
E	T	O141
E	T	O1
E	T	O1
E	T	O1
E	T	O1
E	T	NAg
E	T	O1
E	T	O1
E	T	O1
E	T	O1
E	T	O1

673 **Figure S4. Most human isolates are in a clade distinct from environmental isolates.** The 6 5'

674 IGR sequences of the *V. cholerae* strains described in (31) were used to conduct the maximum

675 likelihood phylogenetic analysis with MEGA. NAg: Non-agglutinating; H: Human isolates; E:

676 Environmental isolates.

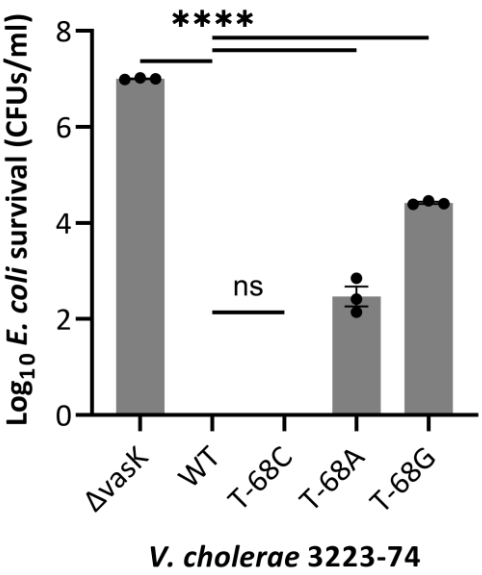

677

678 **Figure S5. Transversions at -68 alter T6 control.** Transversion mutations (T-68A, T-68G) but

679 not a transition mutation (T-68A) introduced into the 3223-74 IGR change T6 control.

680 Competition assays were conducted by co-culturing *V. cholerae* with Cm^R *E. coli* at a ratio of

681 1:10 for 3 h on LB agar plates. Survival *E. coli* was selected by Cm and determined by counts

682 of colony forming units (CFUs). *ΔvasK* in *V. cholerae* prevents assembly of T6 and was served

683 as a $T6^-$ negative control. Data shown are the mean ± S.E. from 3 independent biological

684 replicates. A one-way ANOVA with Dunnett post-hoc test was conducted to determine the

685 significance: ns: not significant, ****$p \leq 0.0001$.

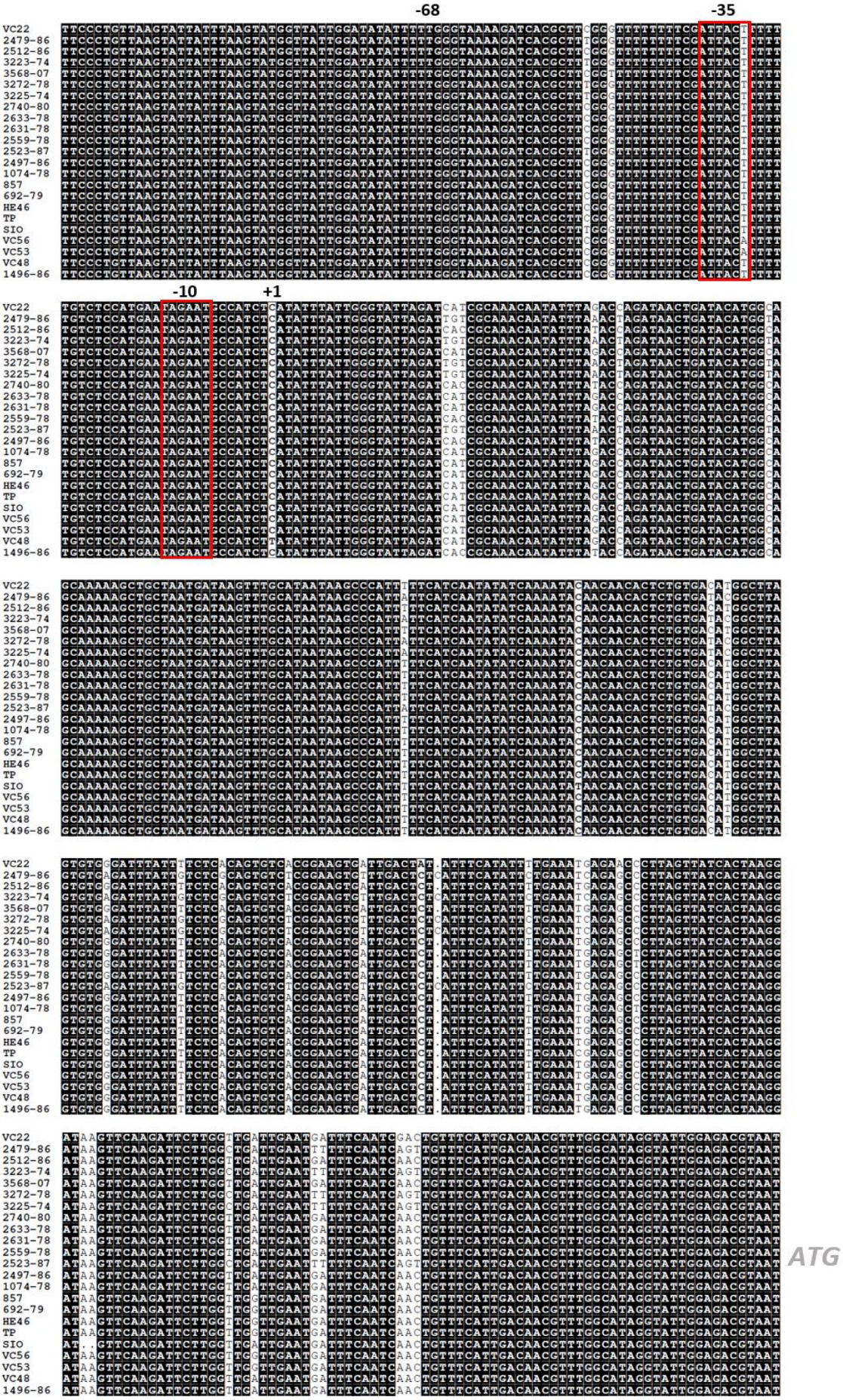
-68
-35
-10
+1
ATG

Figure S6. Alignment of T6 IGR of environmental isolates. Sequences of the *V. cholerae* environmental strains described in (31) were collected from NCBI database (Table S4). The T6 5' IGR sequences were aligned using MUSCLE and generated using ESPript. Conserved bases are highlighted in black, the putative promoter is boxed, and the start codon of *vipA* is in grey.

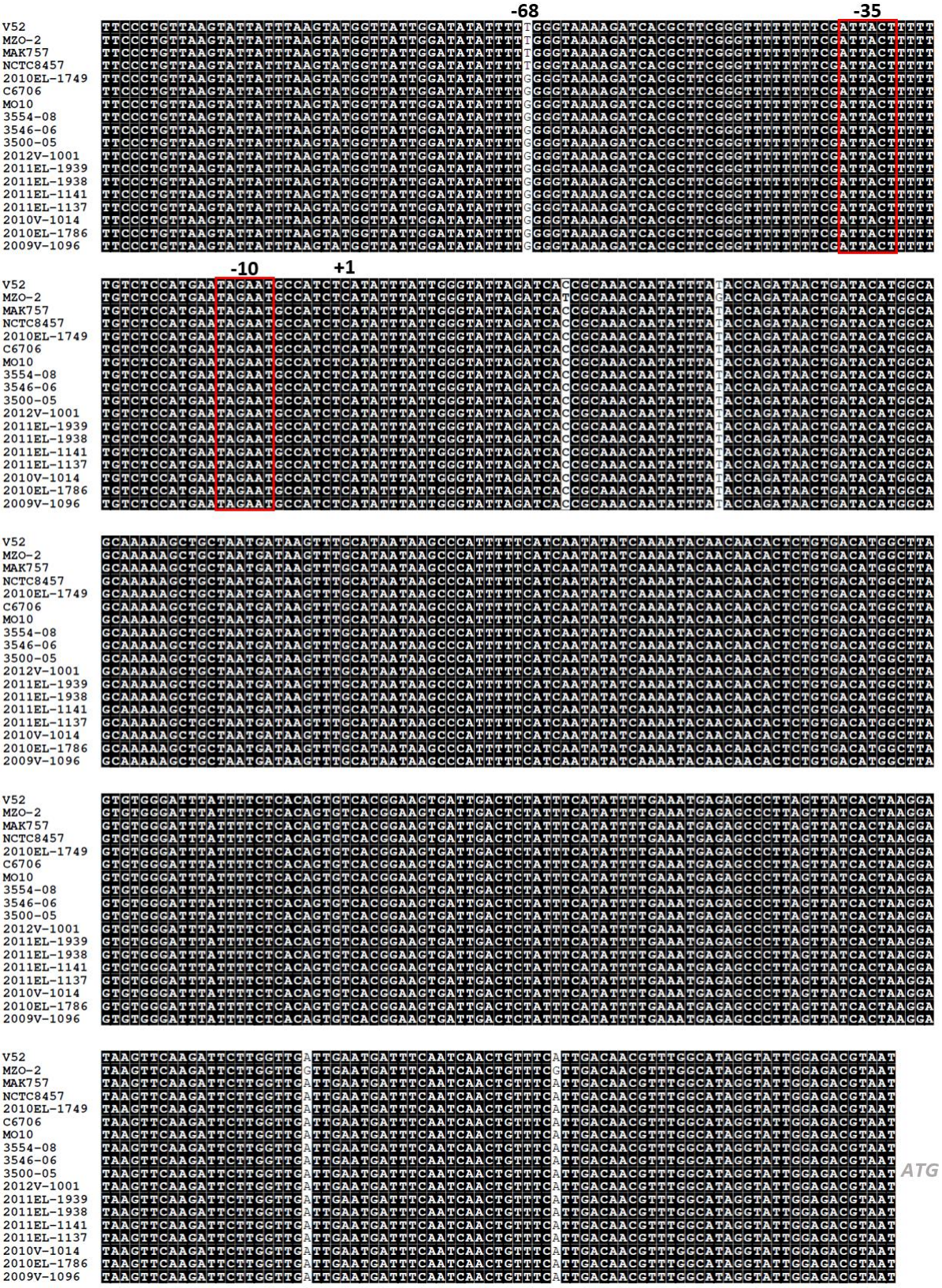

691

692 **Figure S7. Alignment of T6 IGR of human-derived isolates.** Sequences the *V. cholerae* human-

693 derived strains described in (31) were collected from NCBI database (Table S4), except 2012V-

1001, 2011EL-1939, 2011EL-1938, and 2011EL-1141 that were generated by Sanger sequencing. The T6 5’ IGR sequences were aligned using MUSCLE and generated using ESPript. Conserved bases are highlighted in black, the putative promoter is boxed, and the start codon of *vipA* is in grey.